Dual function of MIPS1 as a metabolic enzyme and transcriptional regulator.

David Latrasse, Teddy Jégu, Pin-Hong Meng, Christelle Mazubert, Elodie Hudik, Marianne Delarue, Céline Charon, Martin Crespi, Heribert Hirt, Cécile Raynaud, et al.

Published online 21 January 2013 Nucleic Acids Research, 2013, Vol. 41, No. 5 2907–2917
doi:10.1093/nar/gks1458

Dual function of MIPS1 as a metabolic enzyme and transcriptional regulator

David Latrasse[1], Teddy Jégu[1], Pin-Hong Meng[1,2], Christelle Mazubert[1], Elodie Hudik[1], Marianne Delarue[1], Céline Charon[1], Martin Crespi[3], Heribert Hirt[4], Cécile Raynaud[1], Catherine Bergounioux[1] and Moussa Benhamed[1,*]

[1]Institut de Biologie des Plantes, UMR8618 Université Paris-Sud XI, 91405 Orsay, France, [2]Institute of Horticulture, Guizhou Academy of Agricultural Sciences, GuiYang, Guizhou Province, 550006, P.R. China, [3]Institut des Sciences du Végétal, UPR CNRS, 1 Avenue de la Terrasse, 91198 Gif-sur-Yvette, France and [4]URGV Plant Genomics, INRA/CNRS/University of Evry, 2 rue Gaston Cremieux, 91057 Evry, France

Received July 25, 2012; Revised December 7, 2012; Accepted December 14, 2012

ABSTRACT

Because regulation of its activity is instrumental either to support cell proliferation and growth or to promote cell death, the universal myo-inositol phosphate synthase (MIPS), responsible for myo-inositol biosynthesis, is a critical enzyme of primary metabolism. Surprisingly, we found this enzyme to be imported in the nucleus and to interact with the histone methyltransferases ATXR5 and ATXR6, raising the question of whether MIPS1 has a function in transcriptional regulation. Here, we demonstrate that MIPS1 binds directly to its promoter to stimulate its own expression by locally inhibiting the spreading of ATXR5/6-dependent heterochromatin marks coming from a transposable element. Furthermore, on activation of pathogen response, *MIPS1* expression is reduced epigenetically, providing evidence for a complex regulatory mechanism acting at the transcriptional level. Thus, in plants, MIPS1 appears to have evolved as a protein that connects cellular metabolism, pathogen response and chromatin remodeling.

INTRODUCTION

Although it was first isolated from muscles, myo-inositol (MI) is a ubiquitous compound present in all living organisms. MI is required for the biosynthesis of a huge variety of cellular components, and thereby plays a crucial role in growth and development. In plants, products of MI metabolism are involved in diverse processes such as signal transduction, second messenger signaling, stress response, cell wall biogenesis and chromatin remodeling (1). The rate-limiting step for MI biosynthesis is catalyzed by the MI phosphate synthase (MIPS, E.C.5.5.1.4), and its function has been investigated in various plant species. Loss-of-function studies highlighted the diversity of crucial cellular processes relying on MI. The *Arabidopsis* genome encompasses three isoforms of MIPS, but MIPS1 seems the main player in MI biosynthesis because *mips1* mutants have drastically reduced MI content. *mips1* mutants display pleiotropic defects, including reduced root growth, abnormal vein formation in cotyledons (2,3) and defects in auxin polar transport due to alterations in lipid metabolism (4). However, the most striking feature of *mips1* mutants is the light-dependent formation of lesions on leaves, implicating MIPS1 as a repressor of programmed cell death (2,3). In plants, cellular suicide is required during many steps of development such as xylogenesis (5), plant reproduction (6), leaf and petal senescence (7,8) and root cap and endosperm cell death during germination (9,10). Hence, cell fate can be influenced by differential *MIPS* regulation: its sustained expression is linked to cell proliferation and differentiation, whereas its down-regulation may be involved in the controlled cell death of specific tissues.

Several studies have provided evidence for a role of MIPS in biotic stresses. Indeed, *mips1* mutants display improved resistance toward *Hyaloperonospora arabidopsis*, while *mips3* mutants are more susceptible to a broad range of pathogens, including viruses, virulent and avirulent bacterial strains and the fungus *Botrytis cinerea* (11). Plant defense mechanisms induced by pathogen-associated molecular pattern (PAMP) recognition include hormone signaling via salycilic acid, jasmonic acid and ethylene, regulation of gene expression, strengthening of cell wall reactive oxygen species production and, in some cases, programmed cell death in the case of hypersensitive response (12). Early events of

*To whom correspondence should be addressed. Tel: +33 1 69 15 33 51; Fax: +33 1 69 15 33 24; Email: moussa.benhamed@u-psud.fr

The authors wish it to be known that, in their opinion, the first two authors should be regarded as joint First Authors.

PAMP-induced signaling have been dissected and in the case of bacterial flagellin (flg22), recognition involves two antagonistic MAPK signaling cascades: flagellin recognition by surface receptors triggers the activation of MEKK1, which in turn activates two MAPK modules. One consisting of MKK4/MKK5 and MPK3/MPK6 appears to activate defense genes, whereas the other comprising MKK1/MKK2 and MPK4 would repress them (13). Both *mpk4* and *mkk1/mkk2* mutants display a dwarf phenotype, spontaneous programmed cell death and constitutive activation of pathogen response. Interestingly, the transcriptome of *mips1* mutants is similar to the one of *mpk4* and *mkk1/2* mutants, and expression of *MIPS1* is reduced in these mutants according to publicly available micro-array data, suggesting that *MIPS1* down-regulation may be induced by MAPKs to promote programmed cell death and pathogen resistance. Tight control of *MIPS* expression seems crucial to regulate MI accumulation and localized cell death on biotic stress.

Complex regulation of *MIPS* genes has been found in eukaryotes. In yeast, expression of the *INO1* gene, encoding MIPS, is regulated depending on MI availability by three members of the SWI2/SNF2 class of chromatin remodeling complexes: it is activated in the absence of MI by SWI/SNF, and INO80, whereas it is repressed on MI addition by ISWI (14). In addition, the MI derivatives inositol polyphosphates (IPs) modulate the activity of several ATP-dependent chromatin remodeling complexes. *In vitro* data have shown that NURF-, ISW2- and INO80-stimulated nucleosome mobilization is inhibited by inositol hexakisphosphate (IP_6). On the contrary, inositol tetrakisphosphate (IP_4) and inositol pentakisphosphate (IP_5) stimulate nucleosome mobilization catalyzed by SWI/SNF complex (15). In mammals, the gene encoding MIPS is regulated by DNA methylation (16). Hence, chromatin remodeling appears to be a widespread mechanism regulating *MIPS* expression in many eukaryotes, and similar mechanisms may operate in plants. Interestingly, we showed that the *Arabidopsis* MIPS1 protein interacts with ATXR5 and ATXR6 (2), two histone methyltransferases (HMTs) involved in the methylation of the lysine 27 of histone H3 (17). These observations led us to ask whether MIPS1 itself may be involved in the regulation of its own expression as a part of the plant response to exogenous cues such as pathogen attacks. Indeed, rapid changes in transcript levels, including down-regulation of a gene subset, are triggered by the bacterial elicitor flagellin (18). Pathogen-induced programmed cell death may therefore rely on the repression of *MIPS1* expression via transcriptional mechanisms.

Here we show that in addition to its function as a key enzyme of MI metabolism, MIPS1 controls its own transcription through chromatin changes.

Additionally, regulation of *MIPS1* on flagellin treatment and in *mpk4* mutants points to a role of this mechanism in cell death. This dual function of MIPS1 may ensure *MIPS1* expression under normal growth conditions and its down-regulation on a pathogen attack to induce programmed cell death.

MATERIALS AND METHODS

Plant material and growth conditions

Seeds were surface sterilized by treatment with Bayrochlore (Bayrol) for 20 min, washed and imbibed in sterile water for 2–4 days at 4°C to obtain homogeneous germination. Seeds were sown on commercially available 0.5× Murashige and Skoog medium (Basalt Salt Mixture M0221, Duchefa) solidified with 0.8% agar (Phyto-Agar HP696, Kalys) with the suitable antibiotic if needed and grown in a long-day (16 h light, 8 h night, 21°C) growth chamber. After 2 weeks, the plants were transferred to soil in a greenhouse or in a growth chamber under short-day conditions (8 h light at 20°C, 16 h night at 18°C) for 2 weeks before being transferred to long-day conditions.

RNA extraction and real-time quantitative PCR analysis

Total RNA was extracted from seedlings using the RNeasy MiniPrep kit (Qiagen) according to the manufacturer's instructions. First-strand cDNA was synthesized from 2 µg of total RNA using Improm-II reverse transcriptase (A3802, Promega) according to the manufacturer's instructions. 1/25th of the synthesized cDNA was mixed with 100 nM solution of each primer and LightCycler® 480 Sybr Green I master mix (Roche Applied Science) for quantitative PCR analysis. Products were amplified and fluorescent signals acquired with a LightCycler® 480 detection system. The specificity of amplification products was determined by melting curves. *AtPTF2* was used as internal control for signal normalization. Exor4 relative quantification software (Roche Applied Science) automatically calculates relative expression level of the selected genes with algorithms based on ΔΔCt method. Data were from duplicates of at least two biological replicates. Primers used are described in Supplementary Table S1.

Histochemical β-glucuronidase assays

After 15-min fixation in 80% cold acetone, complete seedlings were stained in Eppendorf tube, and β-glucuronidase (GUS) activity was assayed using 5 mM ferri/ferrocyanide as described (19). After 2 h at 37°C, samples were washed in 70% ethanol for 10 min, and then cleared using chloral hydrate solution (8 g of chloralhydrate, 1 ml of glycerol and 2 ml of water). Images were captured on a microscope Axioskop (Zeiss) with a camera Spot RT slider (Diagnostic instrument) and enhanced using Adobe Photoshop software.

Confocal imaging

Plantlets were mounted in 5% glycerol and directly imaged on a TCS-SP2 upright microscope (Leica Microsystems) with 488-/543-nm excitation, 488-/543-nm beam-splitter filter and 515- to 615-nm (green channel) and 610- to 625-nm (red channel) detection windows. Transmitted light was also collected. All images were acquired with similar gain adjustments.

Chromatin immunoprecipitation analysis

Chromatin immunoprecipitation (ChIP) assays were performed on 12-day-old *in vitro* seedlings using anti- Green Fluorescent Protein (GFP) (Santa Cruz), IgG control (Millipore), anti H3K27me1 (Millipore) or anti-H3K9ac (Millipore) antibodies, using a procedure adapted from Gendrel *et al*. (2005) (20). Briefly, after plant material fixation in 1% (v/v) formaldehyde, tissues were homogenized, and nuclei isolated and lysed. Cross-linked chromatin was sonicated using a water bath Bioruptor UCD-200 (Diagenode, Liège, Belgium) (30 s on/30 s off pulses, at high intensity for 24 min). Protein/DNA complexes were immunoprecipitated with antibodies, overnight at 4°C with gentle shaking, and incubated for 1 h at 4°C with 50 µL of Dynabeads Protein A (Invitrogen, Ref. 100-02D). Immunoprecipitated DNA was then recovered using the IPure kit (Diagenode, Liège, Belgium) and analyzed by quantitative real-time PCR. An aliquot of untreated sonicated chromatin was processed in parallel and used as the total input DNA control. Primers used as described in Supplementary Table S1.

Cell fractionation

14-day-old plantlets were ground to a fine powder in liquid nitrogen. Cells were homogenized and lysed in a buffer on ice (0.5 M sucrose, 15 mM Tris at pH 7.5, 60 mM KCl, 0.25 mM ethylenediaminetetraacetic acid (EDTA), 0.125 mM ethylene glycol tetraacetic acid (EGTA), 0.5 M spermidine, 0.15 mM spermine, 1 mM dithiothreitol). Subsequently, Nonidet P-40 (Sigma) was added to a final concentration of 1%, and lysates were centrifuged to obtain a cytosolic supernatant and nuclear pellet. Nuclei were further purified by centrifugation at 1000*g* through a 0.88 M sucrose cushion.

Transgenic lines generated in this study

The genotypes of the lines used in this work are as follows.

T-DNA insertion lines and their crossings: *mips1-1* (Col0) and *mips1-2* (2) T-DNA insertion lines.

Transgenic lines: *PMIPS1::UidA*, Col0; *PMIPS1::UidA*, Ws; *PMIPS1::UidA*, *mips1-1*, *PMIPS1::UidA*, *mips1-2*; *PMIPS1::UidA*, *ddm1*; *PMIPS1::UidA*, *atxr5 atxr6 mips1-1*.

PMIPS1::MIPS1-GFP (Col0); *PMIPS1::MIPS1-GFP* (*atxr5 atxr6*).

Strains and plasmids

Plasmid PMIPS1::UidA reporter was created by first amplifying the putative *MIPS1* promoter, corresponding to 980 bp upstream of the translation start codon. PCR was performed on genomic DNA isolated from Col0 plants using the following primers: PMIPS1_promoter_Up (5′-CAGAGCAGTAGAAAAAGTGTGAAGA-3′) and PMIPS1_3′down (5′-GCAGAGGAAAAGGAAAATTTGGTTG-3′), and cloned in pGEM-T (Promega). The *PMIPS1* fragment was then digested with SphI and SalI and ligated into the pBI101-UidA. The HindIII–EcoR1 fragment encompassing the *PMIPS1::UidA* fusion and the Nos terminator was then transfered in the binary vector pPZP100 to obtain the PMIPS1::UidA plasmid. The MIPS1-GFP fusion driven by the *PMIPS1* promoter was obtained as follows. First, *PMIPS1-pBI101-UidA* was digested with HindIII and SmaI, and the resulting *PMIPS1* fragment was ligated to pH7WG2 to obtain pH7WG2pMIPS1 (Plant Systems Biology, Vlaams Interuniversitair Instituut voor Biotechnologie, Ghent University) where the *MIPS1* promoter replaces the 35S promoter. Then, the full-length cDNA encoding *AtMIPS1* cloned between the BamHI and XhoI sites of the pENTR1A vector (Invitrogen) was introduced in pH7WG2pMIPS1 by recombination using the Gateway technology (Invitrogen) according to manufacturer's instructions.

Immunoprecipitations

First, expression and purification of Gluthation S-transferase (GST)-ATXR5PHD-SET was performed according to Jacob *et al*. (2009) (21). Second, protein extraction of MIPS1-GFP plantlets was performed. Fourteen-day-old MIPS1-GFP plantlets were ground to a fine powder in liquid nitrogen. Cells were homogenized and lysed in Chris buffer containing 50 mM Tris (pH 8.0), 0.5% Nonidet P-40, 200 mM NaCl, 0.1 mM EDTA, 10% glycerol, 10 mM N-Ethylmaleimide (NEM) and protease inhibitors (Complete EDTA free, Roche).

Total cell lysates were then mixed with GST-tagged ATXR6 and incubated for 2 h at 4°C. MIPS1-GFP was then immunoprecipitated using a monoclonal anti-GFP antibody (Santa Cruz). Immune complexes were collected by incubation for 2 h at 4°C with Protein G plus/Protein A agarose (Pierce) and washed three times in lysis buffer.

Pulled-down proteins were detected by immunoblot using a polyclonal anti-GST antibody or the anti-GFP antibody.

Transient expression

Transient expression in tobacco leaves has been done following the protocol developed by Sparkes *et al*. (2006) (22). Proteins were extracted after 48 h.

Transient expression directly into 7-day-old *Arabidopsis* seedlings after vacuum infiltration of agrobacteria was done according to Marion *et al*. (2008) (23). Plantlets were observed by confocal microscopy after 48 h.

HMT activity

Measurement of HMT activity was performed following EpiQuik HMT Assay Kit instructions (Epigentek P-3005).

Supporting information

Accession numbers

The GenBank accession numbers of the genes and proteins discussed in this article are MIPS1: At4g39800; ATXR5: At5g09790; ATXR6: At5g24330; DCL1: At1g01040; MPK4: At4g01370; and DDM1: At5g66750.

Lines used in this study were T-DNA lines SALK_023626 (*mips1-1*) and Flag_605F08 (*mips1-2*) for *mips1*, SALK_130607 and SAlL_0004263 for *atrx5* and *atrx6* and EMS line for *ddm1* (24).

RESULTS

MIPS1 is required for its own expression

In yeast, expression of the *INO1* gene encoding MIPS is induced when cellular levels of MI are low. To determine whether this regulation was conserved in *Arabidopsis*, we analyzed the transcription of *MIPS1* in *mips1* mutants, which are full knock-outs of the *MIPS1* gene and have a drastic reduction of MI (2). We introduced a construct encompassing a 980-bp genomic fragment upstream of the *MIPS1* start codon fused in-frame to the *uidA* reporter gene encoding GUS (*PMIPS1::uidA*). In wild-type Col0 plants, this construct had a similar expression pattern to the one reported by Donahue *et al*. (2010) (3), using a larger genomic fragment for the *MIPS1* promoter (Figure 1A). Surprisingly, in the *mips1-1* background, GUS staining was weaker than in Col0 in >45 transformed lines (Figure 1A). As silencing frequently occurs in SALK lines derived from Col0 (25), the reduced activity of the *MIPS1* promoter could be an indirect consequence of the T-DNA insertion in the *MIPS1* sequence. We therefore introduced the same construct in the *mips1-2* mutant (2) and in the Ws control to confirm the previous observation in 10 independent lines and discard any silencing effect. Quantification of *uidA* expression levels by qRT-PCR confirmed that in the absence of MIPS1, the *MIPS1* promoter activity was reduced by >10-fold (Figure 1B). MI addition to the growth medium failed to restore normal activity of the *MIPS1* promoter, demonstrating that this MIPS1-mediated regulation was not related to the cellular content in MI, which is consistent with the observation that addition of MI to the growth medium of wild-type plants does not modify *MIPS1* mRNA accumulation (data not shown). To confirm that MIPS1 is required for its own expression, we transiently transformed *mips1-1* mutants with a vector containing *PMIPS1::MIPS1-GFP* and with or without a plasmid containing *35S::MIPS1-RFP*. Confocal microscopy analysis revealed that MIPS1-GFP was expressed in the mutant only when co-transformed with the *35S::MIPS1-RFP* construct (Supplementary Figure S1). These results suggest that the *MIPS1* promoter requires the MIPS1 protein to be active. Hence, the MIPS1 protein may have an unexpected role in the activation of its own transcription.

MIPS1 is localized both in cytoplasm and in nucleus, where it binds to its own promoter

In tobacco BY2 cells, a MIPS1-GFP fusion was localized both in the nuclear and the cytoplasmic compartment (2). This observation can be linked to the presence of a predicted nuclear export signal in the *MIPS1* sequence (Supplementary Figure S2), and supports that MIPS1 could regulate its own expression in the nucleus. To confirm MIPS1 accumulation in the nucleus *in planta*, we analyzed *Arabidopsis* transgenic plants expressing a MIPS1-GFP fusion downstream of the *MIPS1* promoter (*PMIPS1::MIPS1-GFP*). We first checked whether the promoter sequence we used conferred an expression pattern to the reporter gene that is identical to the one reported by Donahue *et al*. (2010) (3). To this end, we took advantage of the plasmids developed by Deal and Henikoff (2011) (26), which allow the expression of GFP targeted to the nuclear envelope under the control of a promoter of interest. Observation of plantlets by confocal microscopy revealed that all leaf cells but only some root cells (Supplementary Figure S3A) were GFP labeled. To quantify this, we next analyzed nuclei extracted from transgenic lines by flow cytometry to estimate the proportion of labeled cells in roots and leaves. As shown in Supplementary Figure S3B, almost all leaf cells (95%) but not all root cells (only 30%) express the *MISP1* gene, which is in agreement with previous observations (3). In addition, the MIPS1-GFP fusion is fully functional, as we demonstrated that it can complement the mutant phenotype (2). GFP localization in the transgenic *PMIPS1::MIPS1-GFP* plants can thus be considered as a good indicator of wild-type MIPS1 protein distribution. Confocal microscopy analysis revealed that the MIPS1-GFP fusion was localized not only mainly in the cytoplasm but also in the nuclei of root cells (Figure 2A). Furthermore, in a cell fractionation experiment (Figure 2B, the small RuBisCO subunit and histone H3 were used as controls for cell fractionation), MIPS1 was detected both in the nuclear and the cytoplasmic compartment, further supporting the hypothesis that MIPS1 could have a nuclear function.

To investigate whether MIPS1 can interact with its own promoter to promote transcription of the *MIPS1* gene, we used ChIP analysis on 12-day-old light-grown seedlings of the *PMIPS1::MIPS1-GFP* plants using GFP antibodies. A marked enrichment of MIPS1 binding on the *MIPS1* promoter (Figure 2C) was found using primers encompassing the whole locus. Hence, the MIPS1 protein is associated to chromatin and binds to its own promoter, suggesting that MIPS1 can directly regulate transcription of *MIPS1*.

MIPS1 interacts with ATXR6 and inhibit its activity *in vitro*

One possible mechanism accounting for the ability of MIPS1 to bind to its own promoter would be through interaction with proteins involved in chromatin remodeling. Indeed, we initially isolated MIPS1 in a yeast two-hybrid screen as an interactor of ATXR5 and ATXR6 (2), two *Arabidopsis* SET [Suvar(3–9), Enhancer of zeste, Trithorax]-domain proteins involved in histone methylation and heterochromatin formation (21). To confirm this interaction, we first performed a co-immunoprecipitation. *PATXR6::ATXR6-GFP* and *PMIPS1::MIPS1-HA* constructs were transfected in tobacco leaves via *Agrobacterium*-mediated infiltration. After protein extraction, ATRX6 or MIPS1 was immunoprecipitated using, respectively, anti-GFP or anti-hyaluronic acid (HA) antibodies (Figure 3A). A band corresponding to GFP-tagged ATXR6 was revealed in the HA immunoprecipitate, and reciprocally a band corresponding to HA-tagged MIPS1 was revealed in the GFP immunoprecipitate (Figure 3A). When the same experiment was performed with leaves transfected

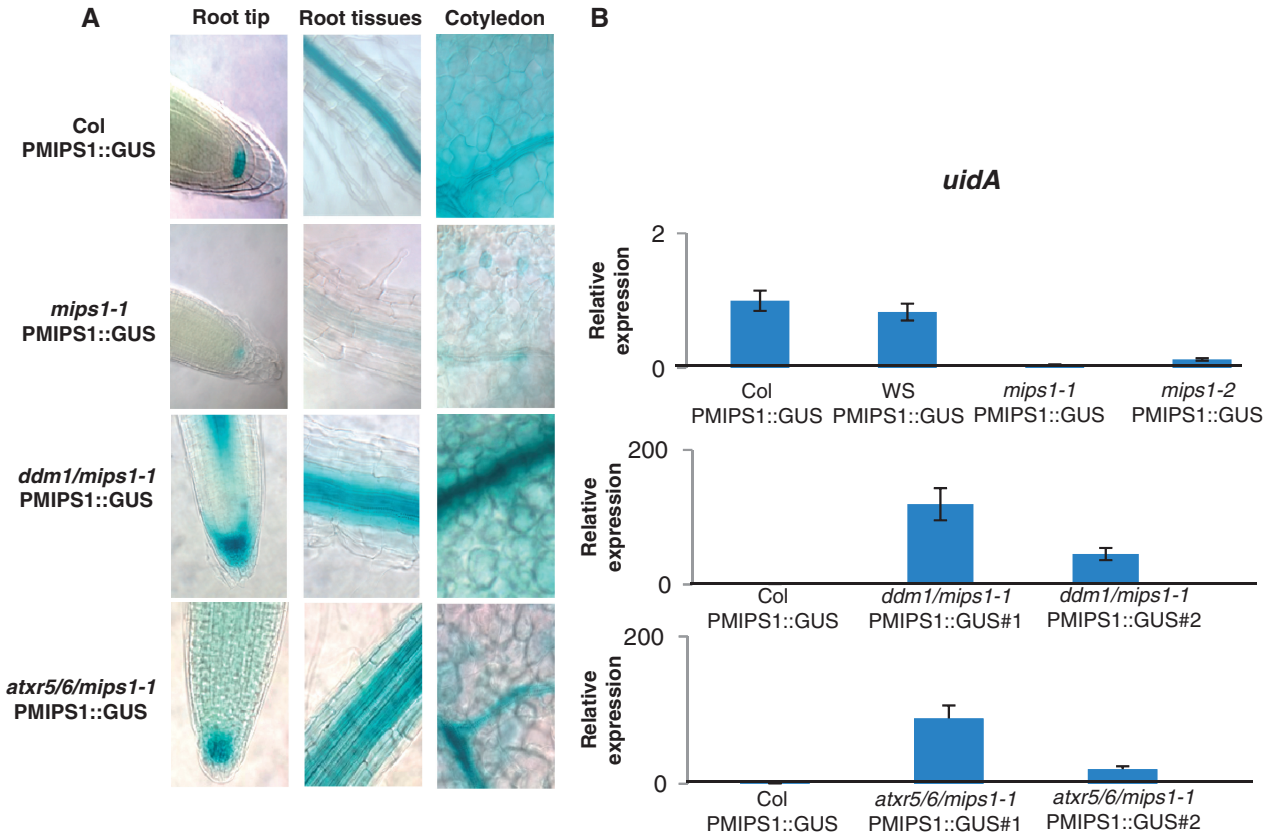

Figure 1. *MIPS1* regulates its own transcription. (**A**) Spatial expression pattern of *MIPS1* promoter in wild-type and different mutant backgrounds (*mips1-1*, *mips1-1*/*ddm1-2* and *mips1-1*/*atxr5*/*6*). Promoter activity was visualized via GUS staining. Root tip: *MIPS1* expression was localized in the first cell layer of the collumella; root tissues: *MIPS1* is mainly expressed in the tissues of the central cylinder; cotyledons: *MIPS1* is strongly expressed in vascular tissues. GUS staining was reduced in the *mips1-1* background but restored both by the *ddm1-2* and *atxr5*/*6* mutations. (**B**) Real-time PCR quantification of the *uidA* reporter expression driven by *MIPS1* promoter in the wild-type and different mutant contexts (*mips1-1, mips1-2*, *mips1-1*/*ddm1-2* and *mips1-1*/*atxr5*/*6*).

only with MIPS1-HA or ATRX6-GFP, no band could be revealed in the GFP precipitate using an HA antibody or in the HA precipitate using the GFP antibody, confirming the specificity of the detected signal in the co-immunoprecipitation assay. This demonstrates that MIPS1 and ATXR6 interact *in planta*. As an independent test, we performed a pull-down experiment. A protein extract from stable transgenic plants expressing a MIPS1-GFP fusion protein was mixed with GST-tagged ATXR6 produced in a bacterial system. MIPS1-GFP was then immunoprecipitated using a monoclonal GFP antibody, and pulled-down proteins were detected by immunoblot using a polyclonal GST antibody (Supplementary Figure S3). A band corresponding to GST-tagged ATXR6 was revealed in the GFP immunoprecipitate (Supplementary Figure S4). All together, our results confirm that MIPS1 and ATXR6 interact and therefore could act in the same complexe(s) *in planta* to regulate *MIPS1* transcription.

ATXR6 is an HMT that catalyzes monomethylation of histone H3 at lysine 27 in *Arabidopsis*. It therefore functions as a repressor of gene expression. One function of the MIPS1 protein could thus be to antagonize the activity of ATXR5 and ATXR6 to allow *MIPS1* expression. To test this hypothesis, we produced ATXR6 *in vitro*, and we measured its HMT activity alone or in the presence of MIPS1-GFP immunoprecipitated from transgenic plants. First, we checked that HMT activity was an increasing function of the ATXR6 quantity (Supplementary Figure S5A). Second, we mixed a constant quantity of ATXR6, which produced the maximum activity with increasing amounts of MIPS1-GFP, and we observed in this condition that HMT activity was a decreasing function of the MIPS1 amount (Supplementary Figure S5B). These results suggest that MIPS1 could inhibit ATXR6 activity *in vitro*.

Expression of *MIPS1* is regulated by ATXR5- and ATXR6-dependent histone modification

To analyze whether MIPS1 regulates its own expression via its ability to modulate ATXR5 and ATXR6 activity, we investigated the role of ATXR5 and ATRX6 proteins in the control of *MIPS1* transcription using the triple mutant *atxr5 atxr6 mips1-1* transformed with *PMIPS1::uidA*. After analysis of GUS staining and quantification of *GUS* transcripts by qRT-PCR, we observed a 20- to 100-fold increase in the transcriptional activity of the *MIPS1* promoter compared with the *mips1-1* background (Figure 1A and B). This result suggests a repressive role of the HMT ATXR5/6 in the control of *MIPS1*

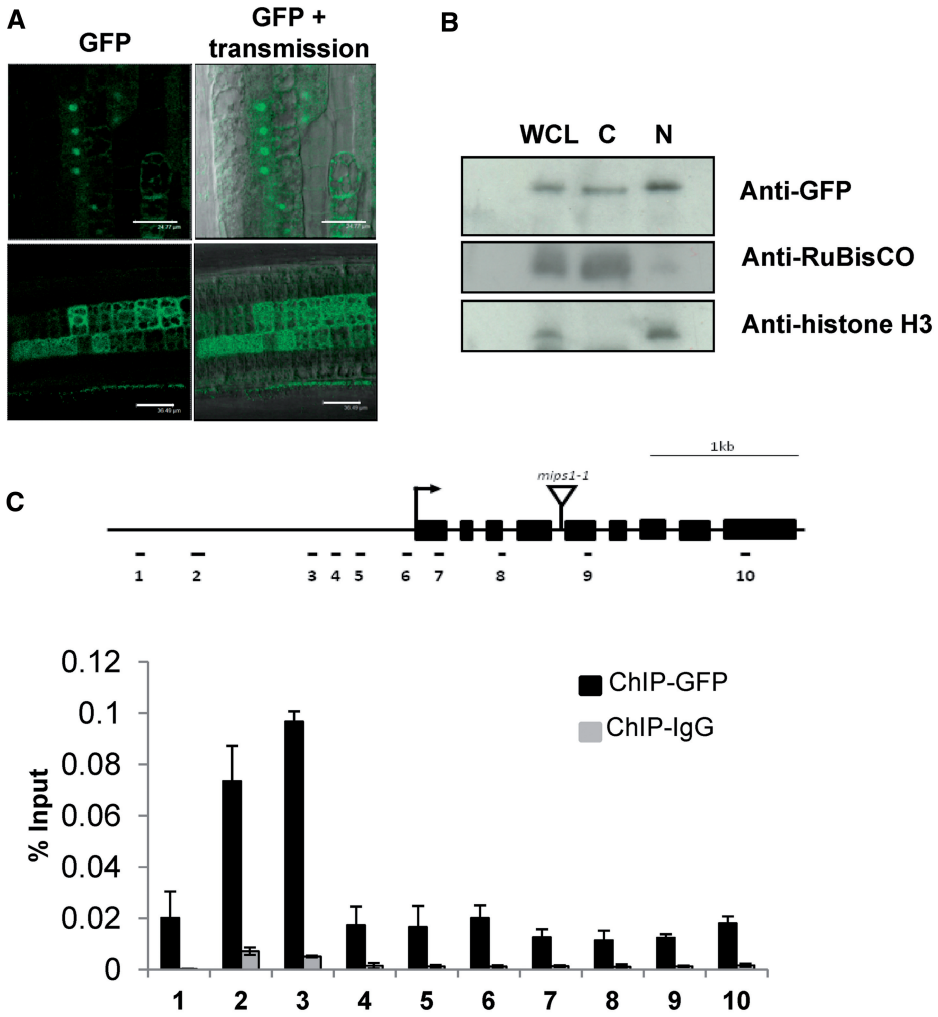

Figure 2. *MIPS1* binds to its own promoter. (**A**) MIPS1-GFP localized both in nuclei and cytoplasm in root cells of Col0 plantlets transformed with the PMIPS1::MIPS1-GFP construct: division zone (upper panel), elongation zone (lower panel). (**B**) Western blot analysis of nuclear and non-nuclear proteins using anti-GFP, anti-RuBisCO and anti-histone H3 antibodies. H3 and RuBisCO were used as positive controls for the nuclear (N) and cytosolic fraction (C), respectively; WCL, whole cell lysate. (**C**) MIPS1 binds to its own promoter. ChIP from *PMIPS1*::*MIPS1-GFP* transgenic plants was performed using anti-GFP (black bars) or anti-IgG antibodies (gray bars). Immunoprecipitated DNA was analyzed by real-time PCR. Graph represents the enrichment of analyzed chromatin fragments relative to input chromatin from wild-type extracts. Black bars, GFP; gray bars, IgG. Error bars represent SD values from at least three repetitions. Position of primer pairs on the *MIPS1* gene is indicated above the graph (open boxes represent the translated regions). T-DNA insertion in *mips1-1* is indicated.

promoter activity, likely through histone modifications. Surprisingly, qRT-PCR analysis revealed that *MIPS1* mRNA accumulation is reduced in *atxr5 atxr6* mutants (Supplementary Figure S6), suggesting an additional level of regulation of *MIPS1* expression at the post-transcriptional level.

To explore more deeply the molecular mechanism of this ATXR5/6-dependent transcriptional repression, we analyzed histone modifications at the *MIPS1* promoter to identify epigenetic marks associated with ATXR5 and ATXR6 activity. *In vitro* characterization of the enzymatic activity of ATXR5 and ATXR6 has previously revealed that these enzymes are H3K27 monomethyltransferases (21). We therefore performed ChIP assays using antibodies raised against monomethylated histone H3K27 on DNA fragments isolated from seedlings of the wild type and *mips1-1*. The enrichment of fragments distributed on the whole locus was compared between *mips1-1* and the wild type (Figure 3B). We observed that monomethylation of H3K27 on the *MIPS1* promoter was significantly increased on the whole locus in the *mips1-1* mutant. This relative increase was particularly marked in the proximal promoter (insert of Figure 3B): indeed, H3K27me1 was increased 1.5- and 1.8-fold in fragments 2 and 3, whereas it was increased 1.8- and 3.5-fold in fragments 5 and 6, respectively. Fragments 2 and 3 are distant from the transcription start site (TSS) of the *MIPS1* gene, but fragments 5 and 6 are in the immediate vicinity of the TSS, which is situated just downstream of fragment 6 (Figure 3B, top): increase of H3K27me1 in the proximal *MIPS1* promoter therefore provides a potential mechanism for the observed reduction of *MIPS1* expression. These data suggested that MIPS1 affects H3K27 methylation of its own promoter by antagonizing ATXR5/6 activity, further demonstrating that ATXR5/6 activity at the *MIPS1* locus is enhanced in the absence of MIPS1.

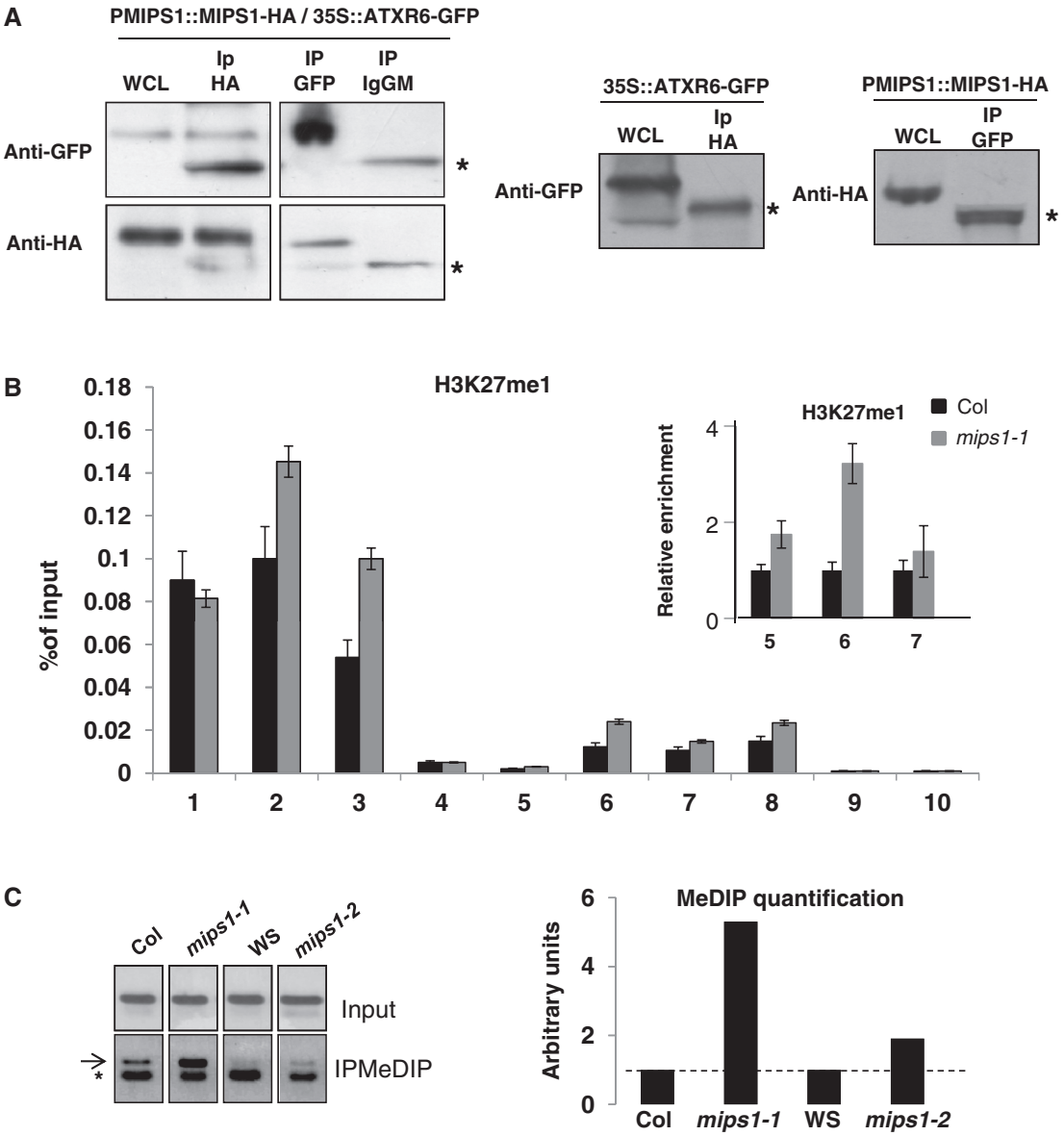

Figure 3. *MIPS1* is epigenetically regulated. (**A**) MIPS1-HA and ATXR6-GFP interact *in vivo*. PATXR6::ATXR6-GFP and PMIPS1::MIPS1-HA constructs were transfected in tobacco leaves via *Agrobacterium*-mediated infiltration. After protein extraction, ATXR6 or MIPS1 was immunoprecipitated using anti-GFP or anti-HA antibodies, respectively, or anti-IgG antibodies as negative controls, and immunoprecipitates were analyzed with anti-GFP and anti-HA antibodies. As positive controls, we used whole cell lysate. The black star indicates IgG. (**B**) Methylation of H3K27 is increased in the *mips1-1* mutant. H3K27me1 state at the whole *MIPS1* locus was analyzed by ChIP on chromatin extracted from Col0 and *mips1-1* plants using an anti-H3K27me1 antibody. Graph represents quantity of ChIP DNA in % of input in Col0 (black bars) and *mips1-1* (grey bars). Error bars represent SD values from at least three repetitions. Insert: because fragments 5 and 6 are situated immediately upstream of the TSS of the MIPS1 gene, we specifically analyzed the relative enrichment in H3K27me1 in the proximal *MIPS1* promoter. Error bars represent SD values from at least three repetitions. Primers used are the same as in Figure 2C. (**C**) Methyl-DNA immunoprecipitation analysis of DNA methylation in Col0, *mips1-1*, Ws and *mips1-2* (arrow indicates the band that is quantified on right; star indicates primer). Quantification after input normalization is showed on the right of the gel.

Taken together, our results demonstrate that transcriptional regulation of *MIPS1* relies on the recruitment of the MIPS1 protein to reduce the deposition of inhibitory histone marks on its own promoter.

Activity of the *MIPS1* promoter is regulated by DNA methylation

The combinatorial analysis of chromatin marks published by Roudier *et al.* (2011) (27) showed that H3K27me1 was often associated with DNA methylation. We then tested whether down-regulation of the *MIPS1* promoter in the *mips1* mutants could involve increased DNA methylation. First, we used zebularine, a cytosine analog, which on incorporation into DNA leads to global DNA demethylation and transcriptional reactivation of epigenetically silent genes and transgenes in *Arabidopsis* (28). Zebularine was applied for 48 h to 10-day-old *mips1-1* plantlets transformed with *PMIPS1::uidA*, and an increase of the *MIPS1* promoter activity was observed in treated lines compared with the non-treated

ones (Supplementary Figure S7). Second, the *mips1-1 PMIPS1::uidA* line was crossed with the *ddm1-2* mutant deficient for the *DDM1* gene encoding an SWI2/SNF2 chromatin remodeling factor, showing a reduction in the DNA methylation level. Both GUS staining and transcript level analysis by qRT-PCR showed that the transcriptional activity of the *MIPS1* promoter is increased by 50- to >100-fold compared with the wild type in the *mips1-1*/*ddm1-2* mutant (Figure 1A and B). Third, we analyzed DNA methylation in the promoter of *MIPS1* by methyl-DNA immunoprecipitation using a monoclonal antibody raised against 5-methylcytidine (5 mC) (Figure 3C). An increase in DNA methylation was observed in *mips1-1* and to a lesser extent in *mips1-2* compared with Col0 and Ws, respectively, indicating that increased H3K27 methylation of the *MIPS1* promoter is indeed associated with increased DNA methylation. Importantly, we found the same regulatory mechanism to operate in the wild-type background because the activity of the *MIPS1* promoter was increased in the *ddm1-2* mutant compared with the wild type (Supplementary Figure S8). These results suggest a direct role of DNA methylation in the control of *MIPS1* promoter activity. As we previously show that expression of the *PMIPS1::uidA* construct is higher in the *atxr5/6* mutant than in the wild type, the deposition of both H3K27me1 and 5mC co-operate in the *mips1* and in the wild-type background to modulate *MIPS1* transcription. We next sought to place this regulatory mechanism in a physiological context.

Flagellin induces a *MIPS1* down-expression through the MPK4 pathway

Disruption of *MIPS1* results in spontaneous cell death, and the transcriptomic profile of *mips1-1* is similar to plants subjected to pathogen infection (2). Induction of programmed cell death during hypersensitive response is a well-known mechanism allowing plant resistance toward pathogens (12). Hence, we postulated that down-regulation of *MIPS1* may be part of the pathogen response of plant cells. We therefore examined *MIPS1* expression in flg22-treated plants. Col0 plantlets were elicited during 1 h with or without 1 μM flagellin, and accumulation of *MIPS1* mRNA was monitored by qRT-PCR. Plants of the Ws ecotype, which lacks the receptor to flg22, were used as a negative control. Accumulation of *MIPS1* transcripts was decreased in flg22-elicited Col0 compared with untreated plantlets or treated Ws plants (Figure 4A). This down-regulation could be due to a transcription inhibition and/or to a decrease of the mRNA stability. Accordingly, *PMIPS1::uidA* plantlets treated with 1 μM flg22 for 1 h showed reduced promoter activity (Figure 4B). These results suggest that *MIPS1* transcription is reduced after flg22 elicitation.

We hypothesized that MIPS1 could act as positive transcriptional regulator of its own expression. To determine whether MIPS1 binding to chromatin correlates with a promoter transcriptional state, we investigated whether MIPS1 could bind to its promoter after flg22 treatment. A ChIP experiment followed by qRT-PCR demonstrated that MIPS1 was released from chromatin after flg22 treatment (Figure 4C). This was accompanied by both a decrease in the euchromatin mark H3K9ac and an increase in the heterochromatin mark H3K27me1 (Figure 4D and E and Supplementary Figure S9), especially in the proximal promoter and first exon of the gene, suggesting that MIPS1 can directly impact the chromatin state of its own promoter after flg22 treatment.

Two MAPK signaling pathways are activated by flg22: MKK4/MKK5–MPK3/MPK6 activates pathogen responses, whereas MEKK1–MPK4 acts negatively on the same responses. To specify the signaling pathway governing *MIPS1* mRNA down-regulation after flg22 treatment, we analyzed the expression of *MIPS1* in the *mpk4* mutant line. qRT-PCR revealed that *MIPS1* is down-regulated in the mutant context (Figure 4). Together, these results suggest that flagellin induces *MIPS1* down-expression through the MPK4 pathway.

DISCUSSION

We previously showed that MIPS1 protects plant cells against cell death under high light intensity or long days (2). In plants, cell death is important for forming body plans and specific organ shapes (29). Therefore, control of *MIPS1* expression would be crucial for plant development. Here we have identified a transcriptional regulation of *MIPS1* expression.

Analysis of *MIPS1* promoter activity in the *mips1* mutant backgrounds or by addition of MI to the growth medium indicates that the MIPS1 protein itself is a positive regulator of *MIPS1* transcription. This hypothesis is in agreement with our previous observation that MIPS1 can accumulate also in the nucleus and can interact with the HMTs ATXR5 and ATXR6 in the yeast two-hybrid system (2). Here we have both confirmed the nuclear localization of MIPS1 and showed that MIPS1 binds to ATXR6 both *in vivo* and *in vitro*. ChIP analysis of the *MIPS1* promoter revealed that ATXR5 and ATXR6 are required for the deposition of H3K27me1, and that this inhibitory mechanism is enhanced in the *mips1* background. This result together with the observation that MIPS1-GFP can bind to the *MIPS1* promoter strongly suggests that MIPS1 itself inhibits ATXR5/6 activity at this locus. This hypothesis is indeed confirmed by the observation that MIPS1 can inhibit ATXR6 activity *in vitro*. MIPS1 recruitment on the *MIPS1* promoter would hence be required to prevent ATXR5/6-dependent histone methylation and associated DNA methylation, thereby allowing normal *MIPS1* transcription. Transcriptionally silent genes often show promoter methylation (30), and genome-wide analysis of chromatin modifications has revealed that DNA methylation and H3K27me1 are often associated in promoters (27). Accordingly, we found DNA methylation to be increased at the *MIPS1* promoter in the *mips1* background. The *MIPS1* locus occupies a sub-telomeric position on chromosome IV, and a Transposable element (TE), present in the distal part of the *MIPS1* promoter, is constitutively methylated

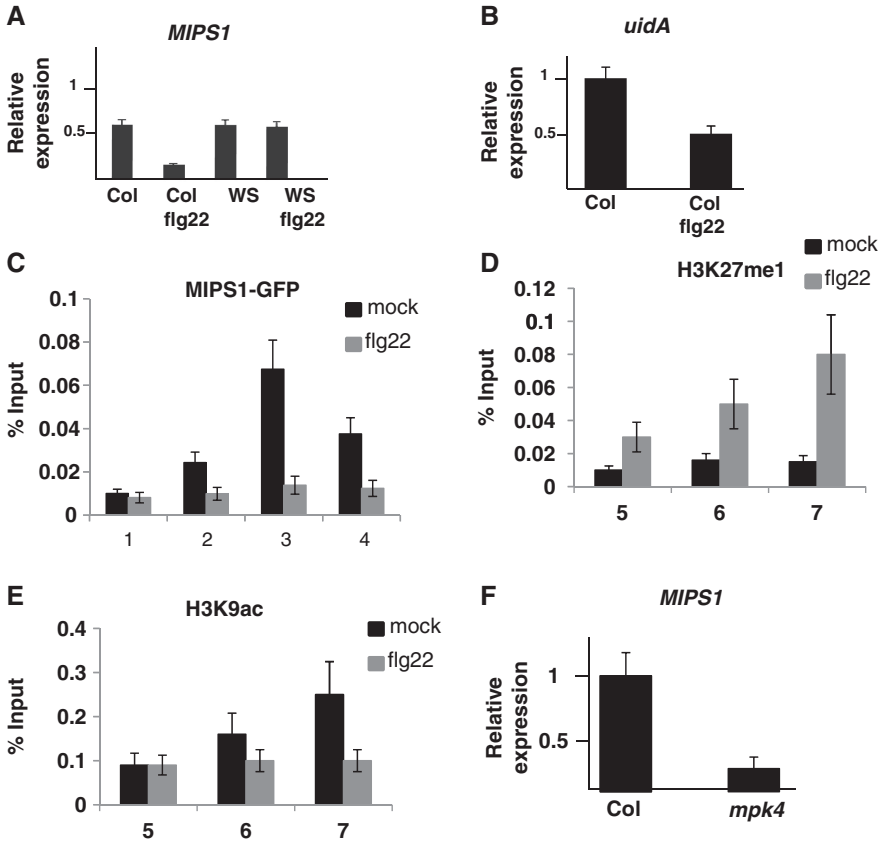

Figure 4. Flagellin induces a *MIPS1* down-expression through the MPK4 pathway. (**A**) Flg22 affects MIPS1 expression. Col0 plantlets were elicited during 1 h with or without 1 μM flagellin; total mRNA was extracted; and real-time PCR was performed. Plants from the Ws ecotype, which is not sensitive to flg22, were used as a negative control. (**B**) *MIPS1* promoter activity is decreased after 1 h of 1 μM flagellin treatment. (**C**) MIPS1 is released on chromatin after flagellin treatment. ChIP assay from *PMIPS1::MIPS1-GFP* transgenic plants treated or not treated with flg22 was performed using an anti-GFP antibody. Immunoprecipitated DNA was analyzed by real-time PCR. Graph represents the enrichment of analyzed chromatin fragments relative to input chromatin. Error bars represent SD values from at least three repetitions. Position of primers pairs on the *MIPS1* gene is indicated above (Figure 2C). (**D**) Methylation of H3K27 increases in the *MIPS1* promoter after flg22 treatment. H3K27me1 state in the proximal *MIPS1* promoter was analyzed by ChIP on chromatin extracted from Col0 treated or not treated with flg22 using an anti-H3K27me1 antibody. Graph represents relative enrichment compared with input. Error bars represent SD values from at least three repetitions. Primers used are the same as in Figure 3B. (**E**) Acetylation of H3K9 decreases in the *MIPS1* promoter after flg22 treatment. H3K9ac state in the proximal *MIPS1* promoter was analyzed by ChIP on chromatin extracted from Col0 treated or not treated with flg22 using an anti-H3K9ac antibody. Graph represents relative enrichment compared with input. Error bars represent SD values from at least three repetitions. Primers used are the same as in (D). (**F**) *MIPS1* is down-regulated in *mpk4* mutants. *MIPS1* mRNA accumulation was quantified by qRT-PCR using Col0 as a control.

at the DNA level and at the H3K27 level (27). Although we cannot rule out that the MIPS1 protein may have an indirect effect on histone methylation in the vicinity of the *MIPS1* gene, its ability to bind to its owm promoter and to inhibit ATXR6 *in vitro* strongly suggests that MIPS1 directly operates at the *MIPS1* locus to prevent heterochromatin spreading from the nearby TE (Figure 5). Indeed, transposable elements have been shown to be involved in local heterochromatin spreading not only in several organisms, including *Drosophila melanogaster* and mouse (31), but also in plant species such as *Brassica napus* (32) or melon, in which a DNA transposon is responsible for the spreading of DNA methylation into the *CmWIP1* promoter, leading to sexual determination (33). H3K27me1 was increased in the absence of *mips1* or on flagellin treatment, especially in the proximal promoter and at the beginning of the coding sequence, suggesting that MIPS1, when associated with the *MIPS1* promoter, functions as a barrier against the propagation of this repressive chromatin mark. The relatively large distance between the peak of MIPS1 fixation in regions 1 and 2, and the region where H3K27me1 is increased in the absence of MIPS1 (regions 6 and 7), may reflect the formation of loop at this locus. Indeed, histone abundance is low in regions 4 and 5, and histone depletion facilitates chromatin loops (Supplementary Figure S10) (34).

The requirement of the MIPS1 protein for *MIPS1* expression is observed even when the *MIPS1* promoter is at an ectopic position in the genome as evidenced by the behavior of the *pMIPS1::GUS* construct or even on a plasmid as observed in transient expression assays. At least two hypotheses can account for this. One possibility would be that ATXR5- and ATXR6-mediated H3K27 methylation is guided by sequence information. Alternatively, the MIPS1 protein may be required to recruit positive regulators of *MIPS1* expression.

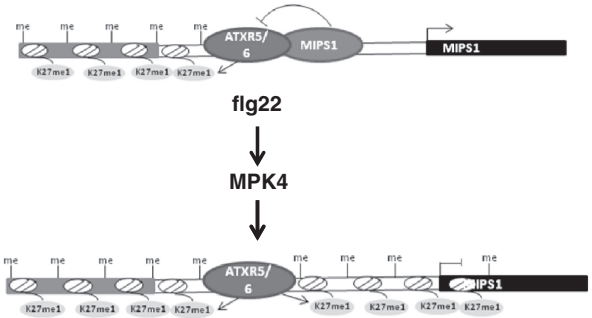

Figure 5. MIPS1 transcriptional regulation model. MIPS1 has a nuclear life and probably can control ATRX5/6 activity to stop the spreading of H3K27me1 coming from a TE present in the distal part of the *MIPS1* promoter. After flg22 treatment, heterochromatin marks coming from the TE can invade the proximal part of the *MIPS1* promoter.

Although the dual function of MIPS1 in MI biosynthesis and transcriptional regulation may seem surprising, a few other examples of enzymes involved both in primary metabolism and chromatin metabolism have been documented. Recently in yeast, homocitrate synthase, which catalyzes the first step of lysine biosynthesis in the cytoplasm, has been shown to play a role in DNA damage repair independent of its catalytic activity (35). Similarly, we did not find any effect of MI in the control of *MIPS1* expression: addition of MI in the growth medium did not restore the activity of the *MIPS1* promoter in the *mips1* mutant, suggesting that the MIPS1 protein itself, but not its catalytic activity, is required for this regulation.

Similarly, ARG5, which catalyzes the second step in ornithine biosynthesis, is also a nuclear and mitochondrial transcription factor (36). Yet another example is the kinase Gal1, which catalyzes a key step in catabolism of galactose and functions as a general activator of GAL gene transcription (37). However, here we showed that MIPS1 intervenes in the control of the epigenetic status of its own promoter.

Data reported here unveiled a complex control of *MIPS1* expression at the transcriptional level, raising the question of the physiological relevance of such sophisticated mechanisms *in planta*. An essential component of *Arabidopsis* biotic stress responses resides in the plant capacity to reprogram its gene expression. Particularly, the stimulation of stress signaling pathway after pathogen attack is integrated into the nucleus through a set of transcription factor, which prioritizes defense over growth-related cellular functions (38). Importance of chromatin modifications and remodeling in the transcriptional regulation of defense-related genes is rapidly emerging (39). Salicylic acid (SA) plays an important role in establishing plant resistance against *Pseudomonas syringae* (40). The SA pathway is substantially controlled by histone modifications. Indeed, the Histone Deacetylase (HDAC) SRT2 suppresses the expression of the SA biosynthetic genes *PAD4*, *EDS5* and *SID2* (41), and loss of HDA19 activity results in enhanced basal expression of many downstream SA-responsive genes (e.g. *PR1*, *PR4* and *PR5*) (42). All together, these reports suggest that chromatin remodeling plays a critical role in the control of *Arabidopsis* defense response. We previously showed that the cell death phenotype of *mips1* is associated with improved resistance to pathogen attack. Thus, plant defense mechanisms may involve *MIPS1* down-regulation to prevent pathogen proliferation. Our findings showed that flg22 treatment results in accumulation of heterochromatin marks on *MIPS1* promoter in *Arabidopsis* and a release of MIPS1 from its own promoter, suggesting that on pathogen attack, MIPS1 is released from chromatin to allow ATXR5/6-dependent silencing of *MIPS1*. Analysis of mutants deficient for PAMP-induced signaling confirmed this hypothesis: the *mpk4* mutant in which SA production and programmed cell death are constitutively activated (13,43) showed also a reduced *MIPS1* expression. Further work will be required to elucidate how MAPK activation induces the release of MIPS1 from chromatin and subsequent reduction in *MIPS1* promoter activity.

In summary, we have established an original picture of *MIPS1* regulation directly involving MIPS1 in the control of its own transcription by inhibition of heterochromatin spreading. Thus, in plants, MIPS1 appears to have evolved as a bifunctional protein that connects cellular metabolism with chromatin functions and provide a new insight in the *MIPS1* function.

SUPPLEMENTARY DATA

Supplementary Data are available at NAR Online: Supplementary Table 1 and Supplementary Figures 1–10.

ACKNOWLEDGEMENTS

The authors are grateful to Hervé Vaucheret (INRA, Versailles) for providing the *ddm1* mutant and to Scott D. Michaels (Department of Biology, Indiana University) for the *atrx5,6* double mutant and for *ATXR6* expression vector. The authors thank Gilles Sante for taking excellent care of our plants and Séverine Domenichini for her expert help in microscopy.

FUNDING

Centre National de la Recherche Scientifique; Université Paris Sud; Agence National de la Recherche (MAPK-IPS ANR-2010-BLAN-1613-02); Program Saclay Plant Sciences (SPS, ANR-10-LABX-40). Funding for open access charge: Université Paris Sud, CNRS and ANR.

Conflict of interest statement. None declared.

REFERENCES

1. Valluru,R. and Van den Ende,W. (2011) Myo-inositol and beyond—emerging networks under stress. *Plant Sci.*, **181**, 387–400.
2. Meng,P.H., Raynaud,C., Tcherkez,G., Blanchet,S., Massoud,K., Domenichini,S., Henry,Y., Soubigou-Taconnat,L., Lelarge-Trouverie,C., Saindrenan,P. *et al.* (2009) Crosstalks between myo-inositol metabolism, programmed cell death and basal immunity in *Arabidopsis*. *PLoS One*, **4**, e7364.

3. Donahue,J.L., Alford,S.R., Torabinejad,J., Kerwin,R.E., Nourbakhsh,A., Ray,W.K., Hernick,M., Huang,X., Lyons,B.M., Hein,P.P. *et al*. (2010) The *Arabidopsis thaliana* Myo-inositol 1-phosphate synthase1 gene is required for Myo-inositol synthesis and suppression of cell death. *Plant Cell*, **22**, 888–903.
4. Luo,Y., Qin,G., Zhang,J., Liang,Y., Song,Y., Zhao,M., Tsuge,T., Aoyama,T., Liu,J., Gu,H. *et al*. (2011) D-myo-inositol-3-phosphate affects phosphatidylinositol-mediated endomembrane function in *Arabidopsis* and is essential for auxin-regulated embryogenesis. *Plant Cell*, **23**, 1352–1372.
5. Fukuda,H. (2000) Programmed cell death of tracheary elements as a paradigm in plants. *Plant Mol. Biol*., **44**, 245–253.
6. Wu,H.M. and Cheun,A.Y. (2000) Programmed cell death in plant reproduction. *Plant Mol. Biol*., **44**, 267–281.
7. Quirino,B.F., Noh,Y.S., Himelblau,E. and Amasino,R.M. (2000) Molecular aspects of leaf senescence. *Trends Plant Sci*., **5**, 278–282.
8. Rubinstein,B. (2000) Regulation of cell death in flower petals. *Plant Mol. Biol*., **44**, 303–318.
9. Fath,A., Bethke,P., Lonsdale,J., Meza-Romero,R. and Jones,R. (2000) Programmed cell death in cereal aleurone. *Plant Mol. Biol*., **44**, 255–266.
10. Young,T.E. and Gallie,D.R. (2000) Programmed cell death during endosperm development. *Plant Mol. Biol*., **44**, 283–301.
11. Murphy,A.M., Otto,B., Brearley,C.A., Carr,J.P. and Hanke,D.E. (2008) A role for inositol hexakisphosphate in the maintenance of basal resistance to plant pathogens. *Plant J*., **56**, 638–652.
12. Coll,N.S., Epple,P. and Dangl,J.L. (2011) Programmed cell death in the plant immune system. *Cell Death Differ*., **18**, 1247–1256.
13. Colcombet,J. and Hirt,H. (2008) *Arabidopsis* MAPKs: a complex signalling network involved in multiple biological processes. *Biochem. J*., **413**, 217–226.
14. Chen,M., Hancock,L.C. and Lopes,J.M. (2007) Transcriptional regulation of yeast phospholipid biosynthetic genes. *Biochim Biophys Acta*, **1771**, 310–321.
15. Shen,X., Xiao,H., Ranallo,R., Wu,W.H. and Wu,C. (2003) Modulation of ATP-dependent chromatin-remodeling complexes by inositol polyphosphates. *Science*, **299**, 112–114.
16. Ratnam,S.S.R.S., Pisano,M.M., Greene,R.M., Casanova,M.F. and Parthasarathy,R.N. (2011) Differential methylation of the gene encoding myo-inositol 3-phosphate synthase (Isyna1) in rat tissues. *Epigenomics*, **3**, 111–124.
17. Jacob,Y., Stroud,H., Leblanc,C., Feng,S., Zhuo,L., Caro,E., Hassel,C., Gutierrez,C., Michaels,S.D. and Jacobsen,S.E. (2010) Regulation of heterochromatic DNA replication by histone H3 lysine 27 methyltransferases. *Nature*, **466**, 987–991.
18. Navarro,L., Zipfel,C., Rowland,O., Keller,I., Robatzek,S., Boller,T. and Jones,J.D. (2004) The transcriptional innate immune response to flg22. Interplay and overlap with Avr gene-dependent defense responses and bacterial pathogenesis. *Plant Physiol*., **135**, 1113–1128.
19. Blazquez,M. (2007) Quantitative GUS activity assay in intact plant tissue. *CSH Protoc*., **2007**, pdb prot4688.
20. Gendrel,A.V., Lippman,Z., Martienssen,R. and Colot,V. (2005) Profiling histone modification patterns in plants using genomic tiling microarrays. *Nat. Methods*, **2**, 213–218.
21. Jacob,Y., Feng,S., LeBlanc,C.A., Bernatavichute,Y.V., Stroud,H., Cokus,S., Johnson,L.M., Pellegrini,M., Jacobsen,S.E. and Michaels,S.D. (2009) ATXR5 and ATXR6 are H3K27 monomethyltransferases required for chromatin structure and gene silencing. *Nat. Struct. Mol. Biol*., **16**, 763–768.
22. Sparkes,I.A., Runions,J., Kearns,A. and Hawes,C. (2006) Rapid, transient expression of fluorescent fusion proteins in tobacco plants and generation of stably transformed plants. *Nat. Protoc*., **1**, 2019–2025.
23. Marion,J., Bach,L., Bellec,Y., Meyer,C., Gissot,L. and Faure,J.D. (2008) Systematic analysis of protein subcellular localization and interaction using high-throughput transient transformation of *Arabidopsis* seedlings. *Plant J*., **56**, 169–179.
24. Mittelsten Scheid,O., Afsar,K. and Paszkowski,J. (1998) Release of epigenetic gene silencing by *trans*-acting mutations in *Arabidopsis*. *Proc. Natl Acad. Sci. USA*, **95**, 632–637.
25. Daxinger,L., Hunter,B., Sheikh,M., Jauvion,V., Gasciolli,V., Vaucheret,H., Matzke,M. and Furner,I. (2008) Unexpected silencing effects from T-DNA tags in *Arabidopsis*. *Trends Plant Sci*., **13**, 4–6.
26. Deal,R.B. and Henikoff,S. (2011) The INTACT method for cell type-specific gene expression and chromatin profiling in *Arabidopsis thaliana*. *Nat. Protoc*., **6**, 56–68.
27. Roudier,F., Ahmed,I., Berard,C., Sarazin,A., Mary-Huard,T., Cortijo,S., Bouyer,D., Caillieux,E., Duvernois-Berthet,E., Al-Shikhley,L. *et al*. (2011) Integrative epigenomic mapping defines four main chromatin states in *Arabidopsis*. *EMBO J*., **30**, 1928–1938.
28. Baubec,T., Pecinka,A., Rozhon,W. and Mittelsten Scheid,O. (2009) Effective, homogeneous and transient interference with cytosine methylation in plant genomic DNA by zebularine. *Plant J*., **57**, 542–554.
29. Lam,E. (2004) Controlled cell death, plant survival and development. *Nat. Rev. Mol. Cell Biol*., **5**, 305–315.
30. Berdasco,M., Alcazar,R., Garcia-Ortiz,M.V., Ballestar,E., Fernandez,A.F., Roldan-Arjona,T., Tiburcio,A.F., Altabella,T., Buisine,N., Quesneville,H. *et al*. (2008) Promoter DNA hypermethylation and gene repression in undifferentiated *Arabidopsis* cells. *PLoS One*, **3**, e3306.
31. Rebollo,R., Karimi,M.M., Bilenky,M., Gagnier,L., Miceli-Royer,K., Zhang,Y., Goyal,P., Keane,T.M., Jones,S., Hirst,M. *et al*. (2011) Retrotransposon-induced heterochromatin spreading in the mouse revealed by insertional polymorphisms. *PLoS Genet*, **7**, e1002301.
32. Arnaud,P., Goubely,C., Pelissier,T. and Deragon,J.M. (2000) SINE retroposons can be used in vivo as nucleation centers for de novo methylation. *Mol. Cell Biol*., **20**, 3434–3441.
33. Martin,A., Troadec,C., Boualem,A., Rajab,M., Fernandez,R., Morin,H., Pitrat,M., Dogimont,C. and Bendahmane,A. (2009) A transposon-induced epigenetic change leads to sex determination in melon. *Nature*, **461**, 1135–1138.
34. Diesinger,P.M., Kunkel,S., Langowski,J. and Heermann,D.W. (2010) Histone depletion facilitates chromatin loops on the kilobasepair scale. *Biophys J*., **99**, 2995–3001.
35. Scott,E.M. and Pillus,L. (2010) Homocitrate synthase connects amino acid metabolism to chromatin functions through Esa1 and DNA damage. *Genes Dev*., **24**, 1903–1913.
36. Hall,D.A., Zhu,H., Zhu,X., Royce,T., Gerstein,M. and Snyder,M. (2004) Regulation of gene expression by a metabolic enzyme. *Science*, **306**, 482–484.
37. Gancedo,C. and Flores,C.L. (2008) Moonlighting proteins in yeasts. *Microbiol. Mol. Biol. Rev*., **72**, 197–210, table of contents.
38. Moore,J.W., Loake,G.J. and Spoel,S.H. (2011) Transcription dynamics in plant immunity. *Plant Cell*, **23**, 2809–2820.
39. Berr,A., Menard,R., Heitz,T. and Shen,W.H. (2012) Chromatin modification and remodelling: a regulatory landscape for the control of *Arabidopsis* defence responses upon pathogen attack. *Cell Microbiol*., **14**, 829–839.
40. Jones,J.D. and Dangl,J.L. (2006) The plant immune system. *Nature*, **444**, 323–329.
41. Wang,C., Gao,F., Wu,J., Dai,J., Wei,C. and Li,Y. (2010) *Arabidopsis* putative deacetylase AtSRT2 regulates basal defense by suppressing PAD4, EDS5 and SID2 expression. *Plant Cell Physiol*., **51**, 1291–1299.
42. Tian,L., Fong,M.P., Wang,J.J., Wei,N.E., Jiang,H., Doerge,R.W. and Chen,Z.J. (2005) Reversible histone acetylation and deacetylation mediate genome-wide, promoter-dependent and locus-specific changes in gene expression during plant development. *Genetics*, **169**, 337–345.
43. Petersen,M., Brodersen,P., Naested,H., Andreasson,E., Lindhart,U., Johansen,B., Nielsen,H.B., Lacy,M., Austin,M.J., Parker,J.E. *et al*. (2000) *Arabidopsis* map kinase 4 negatively regulates systemic acquired resistance. *Cell*, **103**, 1111–1120.